An Effective True-Amplitude Gaussian Beam Migration via Illumination Compensation

S. Liu[1], X. Xie[2], R. Wu[2], Z. Yan[1], H. Gu[1]

[1] China University of Geosciences; [2] University of California

Summary

Conventional migrations are apt to structure imaging, but often incapable of generating true-amplitude subsurface image. We propose a true-amplitude Gaussian beam migration (GBM) method under the framework of seismic illumination compensation. A novel scheme based on the GBM is developed to estimate the point spread functions, with which the illumination compensation can be efficiently implemented in the local wave-number domain. The total computational cost of the proposed true-amplitude imaging includes one Born modelling process and two conventional GBM processes, which is more efficient than the true-amplitude imaging using least squares migration which requires multiple iterations. Numerical examples using synthetic data demonstrated the effectiveness and efficiency of the proposed method.

Introduction

The Gaussian beam migration (GBM) has been widely used for seismic imaging (Cerveny et al., 1982; Hill, 1990; Gray and Bleistein, 2009; Sun et al., 2019). The conventional GBM usually focuses on the geometry of subsurface structures and neglects the amplitude information of the target reflectivity. The GBM can be built into the least-square migration (LSM) by introducing the Born modelling. High-quality images can be obtained by minimizing the misfit between the observed and synthetic data (Hu et al., 2016). The disadvantage of the conventional LSM is that it is very expensive, often requiring 10 to 30 iterations before an acceptable result can be obtained (Schuster and Liu, 2019).

Since the iterative data-fitting in data domain is time-consuming and sometimes hard to converge. There are several non-iterative approaches toward the similar goal by approximating the Hessian matrix and inverse Hessian. Illumination effects resulted from acquisition geometry and overburden structure are proved to be very important in recovering the true reflection amplitude (Wu et al., 2004; Cao and Wu, 2008). From the viewpoint of illumination analysis, true-amplitude imaging is migration with illumination compensation. The compensation can be implemented by ray-based migration (Gelius et al., 2002; Lecomte et al., 2008), one-way wave migration (Wu and Chen, 2006; Xie et al., 2006), and full-wave migration (Yan et al., 2014, Yan and Xie, 2016). From another point of view, both the Hessian matrix and the point spread function (PSF) can be linked to the illumination (Xie and Wu, 2005; Xie et al. 2006; Chen and Xie, 2015). However, efficiently calculating the PSF and applying it in the migration imaging are challenging.

In this study, we propose a true-amplitude GBM imaging method based on illumination compensation. The new method is composed of three steps: 1) Conducting the conventional GBM migration to obtain the image; 2) estimating PSFs using a novel imaging scheme based on the GBM; and 3) applying the PSFs to the conventional image for illumination compensation and obtaining the true-amplitude image.

Gaussian Beam Migration

Gaussian beam method is a high-frequency asymptotic solution for the wave equation. The frequency domain Gaussian beam solution (Hill, 1990) in the ray-centred coordinate can be expressed as

$$u_{\mathrm{GB}}(s,q_1,q_2,\omega)=\sqrt{\frac{v(s)\det \boldsymbol{Q}(s_0)}{v(s_0)\det \boldsymbol{Q}(s)}}\exp\left\{i\omega\left[\tau(s)+\frac{1}{2}\boldsymbol{q}^T[\boldsymbol{P}(s)\boldsymbol{Q}^{-1}(s)]\boldsymbol{q}\right]\right\}, \tag{1}$$

where s and $\boldsymbol{q}^T=(q_1,q_2)$ are ray-centred coordinates, ω is the circular frequency, and s_0 is the initial point of ray. The scalar functions $v(s)$ and $\tau(s)$ are velocity and traveltime along the central ray-path, respectively. The matrix functions $\boldsymbol{P}(s)$ and $\boldsymbol{Q}(s)$ specify the complex dynamic ray parameters, calculated by dynamic ray tracing. The Green's function can be decomposed into a group of Gaussian beams (Gray, 2009; Popov et al., 2010)

$$G(\boldsymbol{x},\boldsymbol{x}_s,\omega)\approx\frac{i\omega}{2\pi}\iint\frac{dp_x^s dp_y^s}{p_z^s}u_{GB}(\boldsymbol{x},\boldsymbol{x}_s,\boldsymbol{p}^s,\omega), \tag{2}$$

where u_{GB} is an individual Gaussian beam in Cartesian coordinates, $\boldsymbol{x}$ is the imaging coordinate, $\boldsymbol{x}_s$ is the coordinate of the source, $\boldsymbol{p}^s=(p_x^s,p_y^s,p_z^s)$ is the slowness vector of the emergence local plane-wave, and the superscript and subscribe s indicate source related parameters. Equation (2) forms the basis for GBM. For implementing the prestack Gaussian beam migration, we use the cross-correlation imaging condition

$$I(\boldsymbol{x})=\frac{-1}{2\pi}\int d\omega\int d\boldsymbol{x}_r\int d\boldsymbol{x}_s\,\frac{\partial G^*(\boldsymbol{x},\boldsymbol{x}_r,\omega)}{\partial z_r}G(\boldsymbol{x},\boldsymbol{x}_s,\omega)D(\boldsymbol{x}_r,\boldsymbol{x}_s,\omega), \tag{3}$$

where $G(\boldsymbol{x},\boldsymbol{x}_s,\omega)$ and $G(\boldsymbol{x},\boldsymbol{x}_r,\omega)$ are background Green's functions calculated using equation (2). They propagate waves from source and receive locations to the image point, respectively. $D(\boldsymbol{x}_r,\boldsymbol{x}_s,\omega)$ is the recorded seismic data in frequency domain, where the subscript r denotes receiver related parameters and the superscript * denotes the complex conjugate.

The point spread function and image correction

The prestack GBM image calculated using equation (3) can be related to the subsurface reflectivity through a PSF in the local wavenumber domain (Xie et al, 2005)

$$I(\boldsymbol{x},\boldsymbol{k}) = R(\boldsymbol{x},\boldsymbol{k})m(\boldsymbol{x},\boldsymbol{k}), \tag{4}$$

where $R(\boldsymbol{x},\boldsymbol{k})$ is the PSF in wavenumber domain, and $m(\boldsymbol{x},\boldsymbol{k})$ is the subsurface reflectivity. We see that the PSF serves as a filter which blurs the reflectivity, converting it into a distorted image. If the localized PSF is available, we can implement the correction by

$$I_c(\boldsymbol{x},\boldsymbol{k}) = I(\boldsymbol{x},\boldsymbol{k}) / R(\boldsymbol{x},\boldsymbol{k}), \tag{6}$$

where I_c is the corrected image.

There are several ways to obtain the localized PSF (Xie et al., 2006; Lecomte, 2008; Cao, 2013; Chen and Xie, 2015; Kang et al., 2019). In this study, we follow the method by Cao (2013) and Chen and Xie (2015), but propose a novel approach to use the GBM to calculate the PSF. Note that equation (4) is a multiplication in the local wavenumber domain, and it is equivalent to a space domain convolution

$$I(\boldsymbol{x},\boldsymbol{x}') = R(\boldsymbol{x},\boldsymbol{x}') * m(\boldsymbol{x},\boldsymbol{x}'), \tag{7}$$

where the convolution is on the local coordinate $\boldsymbol{x}'$. If the $m(\boldsymbol{x},\boldsymbol{x}')$ in (7) is replaced with a single scatterer, which is mathematically a delta function, we have $I(\boldsymbol{x},\boldsymbol{x}') = R(\boldsymbol{x},\boldsymbol{x}')$. In other words, the PSF can be directly obtained by imaging a single scatterer in the background velocity. We introduce the Born modelling (Wu and Aki, 1985) to generate the synthetic data from a point scatterer

$$\mathrm{D}_{delta}(\boldsymbol{x}_r,\boldsymbol{x}_s,\omega) = 2\omega^2\int_D m_{delta}(\boldsymbol{x})\mathrm{G}(\boldsymbol{x},\boldsymbol{x}_s,\omega)\mathrm{G}(\boldsymbol{x},\boldsymbol{x}_r,\omega)\mathrm{d}\boldsymbol{x}, \tag{8}$$

where $m_{delta}(\boldsymbol{x})$ is the model composed of a background and a delta function perturbation. The Gaussian beam Green's function (2) can be used in equation (8). The synthetic data D_{delta} are then used in equation (3) to calculate the image of the scatterer, which is the local PSF $R(\boldsymbol{x},\boldsymbol{x}')$. The space domain PSF can then be converted to the wavenumber domain by perform a local FFT and used in equation (6) for correction, followed by an inverse FFT to transform the corrected imaging back to the space domain. Since the PSF is composed of all factors that affect the image, including the illumination, the correction process deblurs the image and brings it back to the true subsurface reflectivity amplitude.

Numerical Examples

We choose a 5-layer velocity model shown in Figure 1a to test the effectiveness of the proposed method. The size of the model is 4000 m by 9000 m, with a grid spacing of 10 m in both x and z-directions. The four interfaces in the model are numbered T1, T2, T3 and T4, respectively. The synthetic data are generated using a full-wave finite-difference (FD) method, with a 25 Hz Ricker wavelet as the source time function. The acquisition system is composed of 151 surface shots located from 0 to 9000 m at 60 m spacing, and 451 fixed receivers evenly located on the surface with 20 m spacing. To calculate the PSF, we insert 592 point scatterers in the background velocity, followed by implementing the above mentioned process to obtain the PSFs, which are shown in Figure 1b. Note that the PSFs in Figure 1b are in local wavenumber domain. As an example, the inset panel in Figure 1b illustrates one of these PSFs. Next, we perform conventional GBM to produce the subsurface image, which is shown in Figure 1c. We then perform the correction based on these PSFs with equation (6), followed by using the inverse local FFT to obtain the space domain true-amplitude image, which is shown in Figure 1d.

In this specifically designed model, we choose velocities in each layer as a constant. Therefore, the reflectivity on each interface should be a constant. It is clearly seen that, before the correction, the images of these reflectors are highly distorted (Figure 1c). Due to the illumination issue, their amplitudes are weak at where the steep dip exists, or on both left and right sides of the model. After the correction, their amplitudes are mostly recovered (Figure 1d). To further investigate the effect of compensation, amplitudes from 4 reflectors are picked and shown in Figure 2, where the blue and red lines are for normalized amplitudes before and after the correction. Again, the correction brings the amplitudes to nearly the unity. The improvement in the fidelity of the image will considerably benefit the explanation.

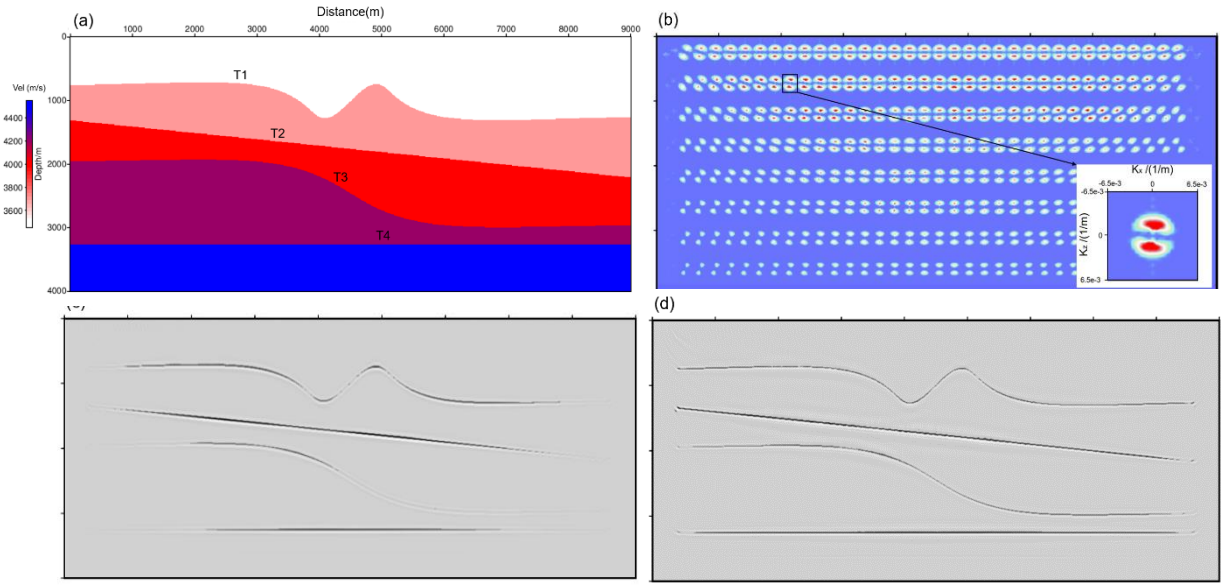

Figure 1. (a) The velocity model for numerical test, where four reflector targets are labelled with T1 to T4. (b) The wavenumber domain PSFs generated using the GBM imaging. (c)The conventional GBM image. (d) The GBM image corrected with the PSF.

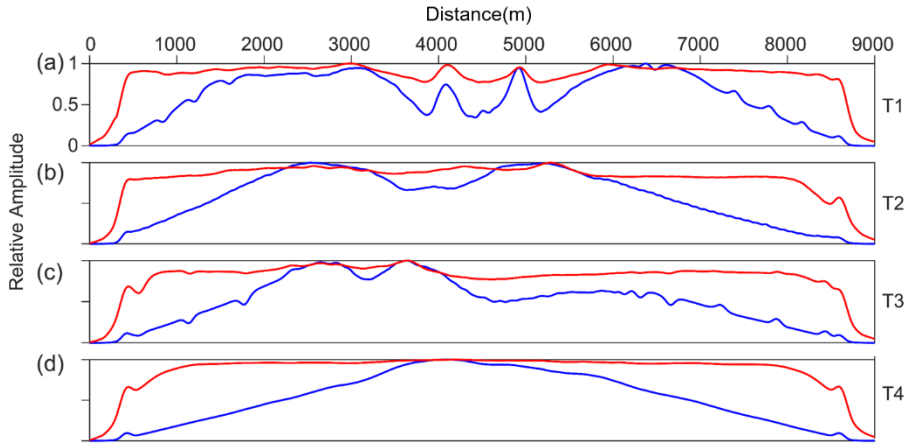

Figure 2. Image amplitudes picked from four reflectors. Shown in (a), (b), (c) and (d) are amplitudes picked from reflectors T1, T2, T3 and T4. The blue and red lines are amplitudes before and after the correction, all normalized to unity.

Discussions

Benefited from the GBM method, PSFs for all inserted scatterers can be calculated simultaneously using the GBM Born modelling and GBM migration, because there are no crosswalks resulted from multiple scatterings between scatterers (Chen and Xie, 2015). This is a merit compared to the full-wave based FD method. Besides, the proposed true-amplitude GBM inherits the merits of ray-based methods, and it has potential to perform with more flexibility (eg., rugged topography acquisition), and it has potential to process the seismic from piedmont areas and the low-fold seismology data. Also, the high-fidelity image can improve the explanation and the corrected image gather can benefit the AVA/AVO calculation.

Conclusion

We propose a true-amplitude GBM method under the frame of illumination compensation. A novel imaging scheme is generated to calculate PSFs based on the GBM, and the illumination compensation can be implemented efficiently with the calculated PSFs. The computational cost of the proposed true-

amplitude imaging method includes one Born modelling process and two migration processes. The current method is more economic than the true-amplitude imaging using the LSM which requires multiple iterations to minimize the data misfit. The numerical test demonstrates that the distorted amplitudes recovered very well after correction.

Acknowledgements

We acknowledge financial supports from the NSFC (41974125) and SINOPEC Key Laboratory of Geophysics (wtyjy-wx2019-01-08). This work is also supported by WTOPI (Wavelet Transform On Propagation and Imaging for seismic exploration) Research Consortium and other funding resources at University of California, Santa Cruz.

References

CAO, J., (2013), *Resolution/illumination analysis and imaging compensation in 3D dip-azimuth domain*,
83rd Annual International Meeting, SEG, Expanded Abstracts, 3931–3936.
CAO, J., and WU R. S. (2008), *Amplitude compensation of one-way wave propagators in inhomogeneous media and its application to seismic imaging*, Commun. Comput. Phys. 3, 203-221.
CERVENY, V., POPOV M.M., and PSENCIK, I. (1982), *Computation of wave fields in inhomogeneous media - Gaussian beam approach*, Geophysical Journal International 70, 109-128.
CHEN, B., XIE, X. B. (2015), *An efficient method for broadband seismic illumination and resolution analyses*, 85th Annual International Meeting, SEG, Expanded Abstracts, 4227–4231.
GELIUS, L.J., LECOMTE, I., and TABTI, H. (2002), *Analysis of the resolution function in seismic prestack depth imaging,*Geophysical Prospecting 50, 505–515.
GRAY, S.H., BLEISTEIN, N. (2009), *True amplitude Gaussian beam migration*, Geophysics 74, S11–S23.
HILL, N. R. (1990), *Gaussian beam migration*, Geophysics 55, 1416–1428.
HU, H., LIU, Y., and ZHENG, Y. (2016), *Least-squares Gaussian beam migration*, Geophysics 81, S87-S100.
KANG, W., WILLINGHAM, B., KIRSEMAN, Z., and YONG, S. L. (2019), *Statistical calibration of the point spread function for image-domain least-squares migration*, 89th Annual International Meeting, SEG, Expanded Abstracts, 4226–4230.
LECOMTE, I. (2008), *Resolution and illumination analyses in PSDM: A ray-based approach*, The Leading Edge 27, 650-663.
SUN, H., GAO, C., and ZHANG, Z. (2019), *High-resolution anisotropic prestack Kirchhoff dynamic focused beam migration*, IEEE Sensors Journal, DOI: 10.1109/JSEN.2019.2933200
SCHUSTER, G., and LIU, Z. (2019), *Least Squares Migration: Current and Future Directions*, 81st Ann. Internat. Mtg., EAGE, We-R11-11
WU, R.S., LUO, M.Q., CHEN, S.C., and XIE, X.B. (2004), *Acquisition aperture correction in angle domain and true-amplitude imaging for wave equation migration*, 74th Annual International Meeting, SEG, Expanded Abstracts, 937–940.
WU, R.S., and Chen, L. (2006), *Directional illumination analysis using beamlet decomposition and propagation*, Geophysics 71, S147-S159.
WU, R.S., and AKI, K. (1985), *Scattering characteristics of waves by an elastic heterogeneity*, Geophysics 50, 582-595.
XIE, X.B., JIN, S., and WU, R.S. (2006), *Wave-equation based seismic illumination analysis*, Geophysics 71, S169-S177.
XIE, X.B., WU, R.S., FEHLER, M., and HUANG, L. (2005), *Seismic resolution and illumination: A wave-equation-based analysis*, 75th Annual International Meeting, SEG, Expanded Abstracts, 1862–1865.
YAN, R., GUAN, H., and XIE, X.B. (2014), *Acquisition aperture correction in the angle domain toward true-reflection reverse time migration*, Geophysics 79, S241-S250.
YAN, Z., and XIE, X.B. (2016), *Full-wave seismic illumination and resolution analyses: A Poynting-vector-based method*, Geophysics 81, S447-S458.